Second Edition

POWER ELECTRONICS

Converters, Applications, and Design

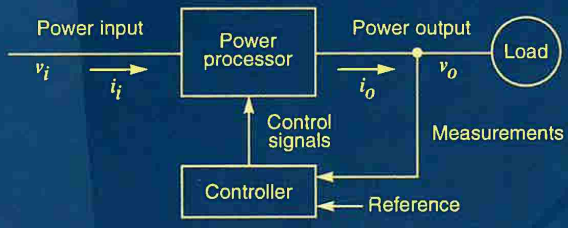

MOHAN / UNDELAND / ROBBINS

ABOUT THE AUTHORS

Ned Mohan is a professor in the Department of Electrical Engineering at the University of Minnesota, where he holds the Oscar A. Schott Chair in Power Electronics. He has worked on several power electronics projects sponsored by the industry and the electric power utilities, including the Electric Power Research Institute. He has numerous publications and patents in this field.

Tore M. Undeland is a Professor in Power Electronics in the Faculty of Electrical Engineering and Computer Science at the Norwegian Institute of Technology. He is also Scientific Advisor to the Norwegian Electric Power Research Institute of Electricity Supply. He has been a visiting scientific worker in the Power Electronics Converter Department of ASEA in Vaasteras, Sweden, and at Siemens in Trondheim, Norway, and a visiting professor in the Department of Electrical Engineering at the University of Minnesota. He has worked on many industrial research and development projects in the power electronics field and has numerous publications.

William P. Robbins is a professor in the Department of Electrical Engineering at the University of Minnesota. Prior to joining the University of Minnesota, he was a research engineer at the Boeing Company. He has taught numerous courses in electronics and semiconductor device fabrication. His research interests are in ultrasonics, pest insect detection via ultrasonics, and micromechanical devices, and he has numerous publications in this field.

POWER ELECTRONICS

Converters, Applications, and Design

SECOND EDITION

NED MOHAN
Department of Electrical Engineering
University of Minnesota
Minneapolis, Minnesota

TORE M. UNDELAND
Faculty of Electrical Engineering and Computer Science
Norwegian Institute of Technology
Trondheim, Norway

WILLIAM P. ROBBINS
Department of Electrical Engineering
University of Minnesota
Minneapolis, Minnesota

JOHN WILEY & SONS, INC.
New York Chichester Brisbane Toronto Singapore

Acquisitions Editor	Steven M. Elliot
Developmental Editor	Sean M. Culhane
Marketing Manager	Susan Elbe
Senior Production Editor	Savoula Amanatidis
Text Designer	Lynn Rogan
Cover Designer	David Levy
Manufacturing Manager	Lori Bulwin
Illustration Coordinator	Jaime Perea

This book was typeset in Times Roman by The Clarinda Company, and printed and bound by Hamilton Printing Company. The cover was printed by NEBC.

Recognizing the importance of preserving what has been written, it is a policy of John Wiley & Sons, Inc. to have books of enduring value published in the United States printed on acid-free paper, and we exert our best efforts to that end.

PSpice is a registered trademark of MicroSim Corporation.
MATLAB is a registered trademark of The MathWorks, Inc.

Library of Congress Cataloging in Publication Data:

Mohan, Ned.
Power electronics : converters, applications, and design / Ned Mohan, Tore M. Undeland, William P. Robbins.—2nd ed.
p. cm.
Includes bibliographical references and indexes.
ISBN 0-471-58408-8 (cloth)
1. Power electronics. 2. Electric current converters. 3. Power semiconductors. I. Undeland, Tore M. II. Robbins, William P. III. Title.
TK7881.15.M64 1995
621.317—dc20 94-21158
CIP

Printed in the United States of America.

10 9 8 7 6 5 4 3 2

PREFACE

SECOND EDITION

The first edition of this book was published in 1989. The basic intent of this edition remains the same; that is, as a cohesive presentation of power electronics fundamentals for applications and design in the power range of 500 kW or less, where a huge market exists and where the demand for power electronics engineers is likely to be. Based on the comments collected over a five-year period, we have made a number of substantial changes to the text. The key features are as follows:

- An introductory chapter has been added to provide a review of basic electrical and magnetic circuit concepts, making it easier to use this book in introductory power electronics courses.
- A chapter on computer simulation has been added that describes the role of computer simulations in power electronics. Examples and problems based on PSpice® and MATLAB® are included. However, we have organized the material in such a way that any other simulation package can be used instead or the simulations can be skipped altogether.
- Unlike the first edition, the diode rectifiers and the phase-controlled thyristor converters are covered in a complete and easy-to-follow manner. These two chapters now contain 56 problems.
- A new chapter on the design of inductors and transformers has been added that describes easy-to-understand concepts for step-by-step design procedures. This material will be extremely useful in introducing the design of magnetics into the curriculum.
- A new chapter on heat sinks has been added.

ORGANIZATION OF THE BOOK

This book is divided into seven parts. Part 1 presents an introduction to the field of power electronics, an overview of power semiconductor switches, a review of pertinent electric and magnetic circuit concepts, and a generic discussion of the role of computer simulations in power electronics.

Part 2 discusses the generic converter topologies that are used in most applications. The actual semiconductor devices (transistors, diodes, and so on) are assumed to be ideal, thus allowing us to focus on the converter topologies and their applications.

Part 3 discusses switch-mode dc and uninterruptible power supplies. Power supplies represent one of the major applications of power electronics.

Part 4 considers motor drives, which constitute another major applications area.

Part 5 includes several industrial and commercial applications in one chapter. Another chapter describes various high-power electric utility applications. The last chapter in this part of the book examines the harmonics and electromagnetic interference concerns and remedies for interfacing power electronic systems with the electric utilities.

Part 6 discusses the power semiconductor devices used in power electronic converters including diodes, bipolar junction thyristors, metal–oxide–semiconductor (MOS) field effect transistors, thyristors, gate turn-off thyristors, insulated gate bipolar transistors, and MOS-controlled thyristors.

Part 7 discusses the practical aspects of power electronic converter design including snubber circuits, drive circuits, circuit layout, and heat sinks. An extensive new chapter on the design of high-frequency inductors and transformers has been added.

PSPICE SIMULATIONS FOR TEACHING AND DESIGN

As a companion to this book, a large number of computer simulations are available directly from Minnesota Power Electronics Research and Education, P.O. Box 14503, Minneapolis, MN 55414 (Phone/Fax: 612-646-1447) to aid in teaching and in the design of power electronic systems. The simulation package comes complete with a diskette with 76 simulations of power electronic converters and systems using the classroom (evaluation) version of PSpice for IBM-PC-compatible computers, a 261-page detailed manual that describes each simulation and a number of associated exercises for home assignments and self-learning, a 5-page instruction set to illustrate PSpice usage using these simulations as examples, and two high-density diskettes containing a copy of the classroom (evaluation) version of PSpice. This package (for a cost of $395 plus a postage of $4 within North America and $25 outside) comes with a site license, which allows it to be copied for use at a single site within a company or at an educational institution in regular courses given to students for academic credits.

SOLUTIONS MANUAL

As with the first edition of this book, a solutions manual with completely worked-out solutions to all the problems is available from the publisher.

ACKNOWLEDGMENTS

We wish to thank all the instructors who have allowed us this opportunity to write the second edition of our book by adopting its first edition. Their comments have been most useful. We are grateful to Professors Peter Lauritzen of the University of Washington, Thomas Habetler of the Georgia Institute of Technology, Daniel Chen of the Virginia Institute of Technology, Alexander Emanuel of the Worcester Polytechnic Institute, F. P. Dawson of the University of Toronto, and Marian Kazimierczuk of the Wright State University for their helpful suggestions in the second edition manuscript. We express our sincere appreciation to the Wiley editorial staff, including Steven Elliot, Sean Culhane, Lucille Buonocore, and Savoula Amanatidis, for keeping us on schedule and for many spirited discussions.

Ned Mohan
Tore M. Undeland
William P. Robbins

CONTENTS

CHAPTER 7

dc–dc SWITCH-MODE CONVERTERS

7-1 INTRODUCTION

The dc–dc converters are widely used in regulated switch-mode dc power supplies and in dc motor drive applications. As shown in Fig. 7-1, often the input to these converters is an unregulated dc voltage, which is obtained by rectifying the line voltage, and therefore it will fluctuate due to changes in the line-voltage magnitude. Switch-mode dc-to-dc converters are used to convert the unregulated dc input into a controlled dc output at a desired voltage level.

Looking ahead to the application of these converters, we find that these converters are very often used with an electrical isolation transformer in the switch-mode dc power supplies and almost always without an isolation transformer in case of dc motor drives. Therefore, to discuss these circuits in a generic manner, only the nonisolated converters are considered in this chapter, since the electrical isolation is an added modification.

The following dc–dc converters are discussed in this chapter:

1. Step-down (buck) converter
2. Step-up (boost) converter
3. Step-down/step-up (buck–boost) converter
4. Cúk converter
5. Full-bridge converter

Of these five converters, only the step-down and the step-up are the basic converter topologies. Both the buck–boost and the Cúk converters are combinations of the two basic topologies. The full-bridge converter is derived from the step-down converter.

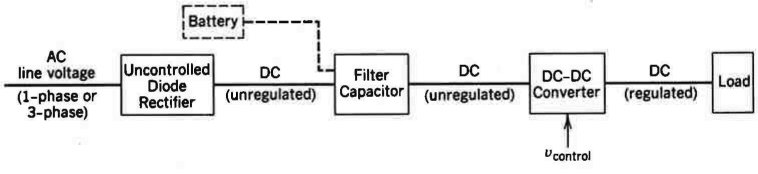

Figure 7-1 A dc–dc converter system.

The converters listed are discussed in detail in this chapter. Their variations, as they apply to specific applications, are described in the chapters dealing with switch-mode dc power supplies and dc motor drives.

In this chapter, the converters are analyzed in steady state. The switches are treated as being ideal, and the losses in the inductive and the capacitive elements are neglected. Such losses can limit the operational capacity of some of these converters and are discussed separately.

The dc input voltage to the converters is assumed to have zero internal impedance. It could be a battery source; however, in most cases, the input is a diode rectified ac line voltage (as is discussed in Chapter 5) with a large filter capacitance, as shown in Fig. 7-1 to provide a low internal impedance and a low-ripple dc voltage source.

In the output stage of the converter, a small filter is treated as an integral part of the dc-to-dc converter. The output is assumed to supply a load that can be represented by an equivalent resistance, as is usually the case in switch-mode dc power supplies. A dc motor load (the other application of these converters) can be represented by a dc voltage in series with the motor winding resistance and inductance.

7-2 CONTROL OF dc–dc CONVERTERS

In dc–dc converters, the average dc output voltage must be controlled to equal a desired level, though the input voltage and the output load may fluctuate. Switch-mode dc–dc converters utilize one or more switches to transform dc from one level to another. In a dc–dc converter with a given input voltage, the average output voltage is controlled by controlling the switch on and off durations (t_{on} and t_{off}). To illustrate the switch-mode conversion concept, consider a basic dc–dc converter shown in Fig. 7-2*a*. The average value V_o of the output voltage v_o in Fig. 7-2*b* depends on t_{on} and t_{off}. One of the methods for controlling the output voltage employs switching at a constant frequency (hence, a constant switching time period $T_s = t_{on} + t_{off}$) and adjusting the on duration of the switch to control the average output voltage. In this method, called *pulse-width modulation* (PWM) switching, the switch duty ratio D, which is defined as the ratio of the on duration to the switching time period, is varied.

The other control method is more general, where both the switching frequency (and hence the time period) and the on duration of the switch are varied. This method is used only in dc–dc converters utilizing force-commutated thyristors and therefore will not be discussed in this book. Variation in the switching frequency makes it difficult to filter the ripple components in the input and the output waveforms of the converter.

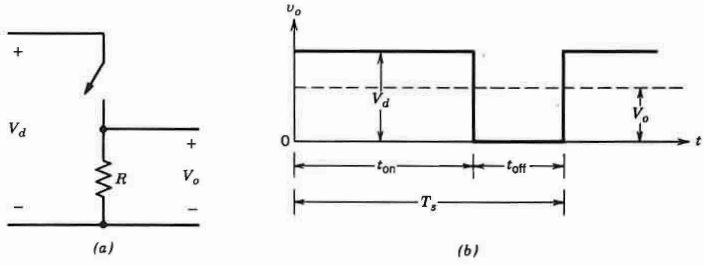

Figure 7-2 Switch-mode dc–dc conversion.

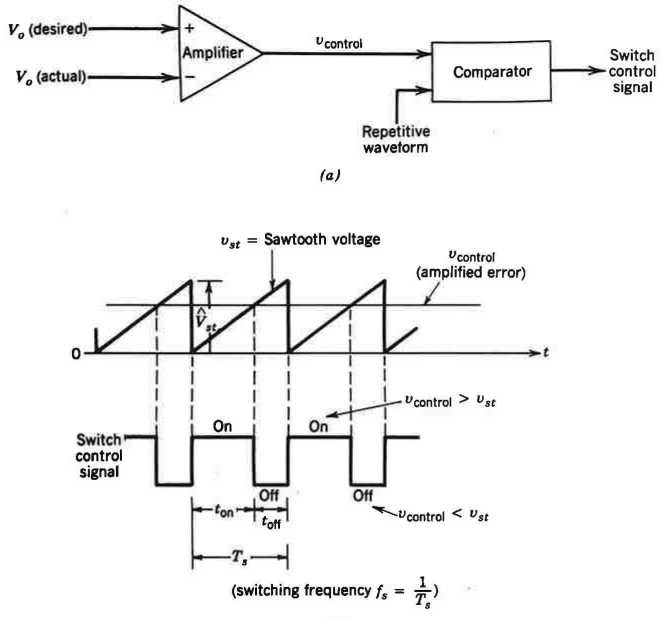

Figure 7-3 Pulse-width modulator: (*a*) block diagram; (*b*) comparator signals.

In the PWM switching at a constant switching frequency, the switch control signal, which controls the state (on or off) of the switch, is generated by comparing a signal-level control voltage $v_{control}$ with a repetitive waveform as shown in Figs. 7-3*a* and 7-3*b*. The control voltage signal generally is obtained by amplifying the error, or the difference between the actual output voltage and its desired value. The frequency of the repetitive waveform with a constant peak, which is shown to be a sawtooth, establishes the switching frequency. This frequency is kept constant in a PWM control and is chosen to be in a few kilohertz to a few hundred kilohertz range. When the amplified error signal, which varies very slowly with time relative to the switching frequency, is greater than the sawtooth waveform, the switch control signal becomes high, causing the switch to turn on. Otherwise, the switch is off. In terms of $v_{control}$ and the peak of the sawtooth waveform $\hat{V}_{st}$ in Fig. 7-3, the switch duty ratio can be expressed as

$$D = \frac{t_{on}}{T_s} = \frac{v_{control}}{\hat{V}_{st}} \tag{7-1}$$

The dc–dc converters can have two distinct modes of operation: (1) continuous current conduction and (2) discontinuous current conduction. In practice, a converter may operate in both modes, which have significantly different characteristics. Therefore, a converter and its control should be designed based on both modes of operation.

7-3 STEP-DOWN (BUCK) CONVERTER

As the name implies, a step-down converter produces a lower average output voltage than the dc input voltage V_d. Its main application is in regulated dc power supplies and dc motor speed control.

Conceptually, the basic circuit of Fig. 7-2*a* constitutes a step-down converter for a purely resistive load. Assuming an ideal switch, a constant instantaneous input voltage V_d, and a purely resistive load, the instantaneous output voltage waveform is shown in Fig. 7-2*b* as a function of the switch position. The average output voltage can be calculated in terms of the switch duty ratio:

$$V_o = \frac{1}{T_s}\int_0^{T_s} v_o(t)\,dt = \frac{1}{T_s}\left(\int_0^{t_{on}} V_d\,dt + \int_{t_{on}}^{T_s} 0\,dt\right) = \frac{t_{on}}{T_s}V_d = DV_d \qquad (7\text{-}2)$$

Substituting for D in Eq. 7-2 from Eq. 7-1 yields

$$V_o = \frac{V_d}{\hat{V}_{st}} v_{control} = kv_{control}$$

where

$$k = \frac{V_d}{\hat{V}_{st}} = \text{constant}$$

By varying the duty ratio t_{on}/T_s of the switch, V_o can be controlled. Another important observation is that the average output voltage V_o varies linearly with the control voltage, as is the case in linear amplifiers. In actual applications, the foregoing circuit has two drawbacks: (1) In practice the load would be inductive. Even with a resistive load, there would always be certain associated stray inductance. This means that the switch would have to absorb (or dissipate) the inductive energy and therefore it may be destroyed. (2) The output voltage fluctuates between zero and V_d, which is not acceptable in most applications. The problem of stored inductive energy is overcome by using a diode as shown in Fig. 7-4*a*. The output voltage fluctuations are very much diminished by using a low-pass filter, consisting of an inductor and a capacitor. Figure 7-4*b* shows the waveform of the input v_{oi} to the low-pass filter (same as the output voltage in Fig. 7-2*b* without a low-pass filter), which consists of a dc component V_o, and the harmonics at the switching frequency f_s and its multiples, as shown in Fig. 7-4*b*. The low-pass filter characteristic with the damping provided by the load resistor R is shown in Fig. 7-4*c*. The corner frequency f_c of this low-pass filter is selected to be much lower than the switching frequency, thus essentially eliminating the switching frequency ripple in the output voltage.

During the interval when the switch is on, the diode in Fig. 7-4*a* becomes reverse biased and the input provides energy to the load as well as to the inductor. During the interval when the switch is off, the inductor current flows through the diode, transferring some of its stored energy to the load.

In the steady-state analysis presented here, the filter capacitor at the output is assumed to be very large, as is normally the case in applications requiring a nearly constant instantaneous output voltage $v_o(t) \simeq V_o$. The ripple in the capacitor voltage (output voltage) is calculated later.

From Fig. 7-4*a* we observe that in a step-down converter, the average inductor current is equal to the average output current I_o, since the average capacitor current in steady state is zero (as discussed in Chapter 3, Section 3-2-5-1).

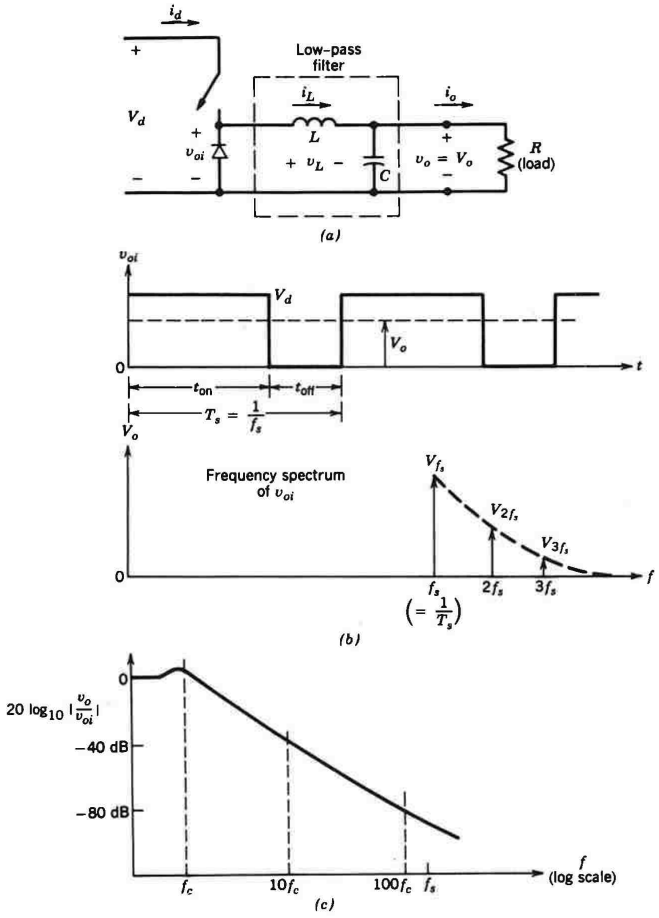

Figure 7-4 Step-down dc–dc converter.

7-3-1 CONTINUOUS-CONDUCTION MODE

Figure 7-5 shows the waveforms for the continuous-conduction mode of operation where the inductor current flows continuously [$i_L(t) > 0$]. When the switch is on for a time duration t_{on}, the switch conducts the inductor current and the diode becomes reverse biased. This results in a positive voltage $v_L = V_d - V_o$ across the inductor in Fig. 7-5*a*. This voltage causes a linear increase in the inductor current i_L. When the switch is turned off, because of the inductive energy storage, i_L continues to flow. This current now flows through the diode, and $v_L = -V_o$ in Fig. 7-5*b*.

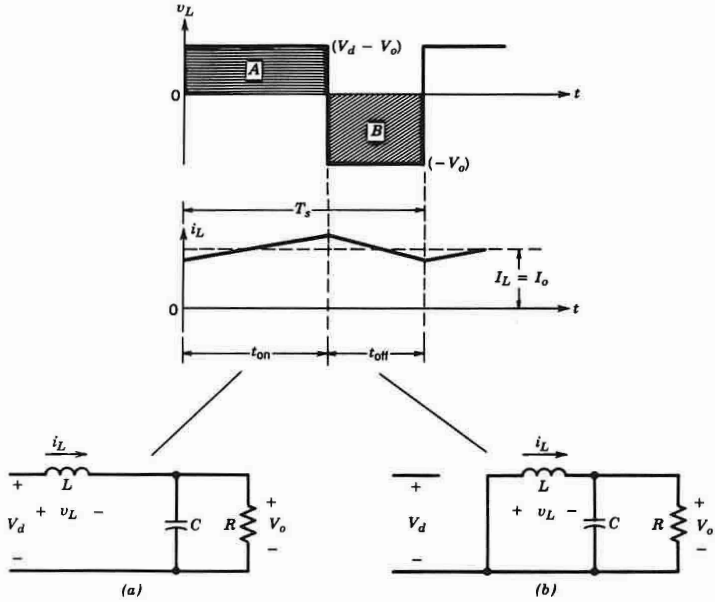

Figure 7-5 Step-down converter circuit states (assuming i_L flows continuously): (*a*) switch on; (*b*) switch off.

Since in steady-state operation the waveform must repeat from one time period to the next, the integral of the inductor voltage v_L over one time period must be zero, as discussed in Chapter 3 (Eq. 3-51), where $T_s = t_{on} + t_{off}$:

$$\int_0^{T_s} v_L \, dt = \int_0^{t_{on}} v_L \, dt + \int_{t_{on}}^{T_s} v_L \, dt = 0$$

In Fig. 7-5, the foregoing equation implies that the areas A and B must be equal. Therefore,

$$(V_d - V_o)t_{on} = V_o(T_s - t_{on})$$

or

$$\frac{V_o}{V_d} = \frac{t_{on}}{T_s} = D \quad \text{(duty ratio)} \tag{7-3}$$

Therefore, in this mode, the voltage output varies linearly with the duty ratio of the switch for a given input voltage. It does not depend on any other circuit parameter. The foregoing equation can also be derived by simply averaging the voltage v_{oi} in Fig. 7-4*b* and recognizing that the average voltage across the inductor in steady-state operation is zero:

$$\frac{V_d t_{on} + 0 \cdot t_{off}}{T_s} = V_o$$

or

$$\frac{V_o}{V_d} = \frac{t_{on}}{T_s} = D$$

Neglecting power losses associated with all the circuit elements, the input power P_d equals the output power P_o:

$$P_d = P_o$$

Therefore,

$$V_d I_d = V_o I_o$$

and

$$\frac{I_o}{I_d} = \frac{V_d}{V_o} = \frac{1}{D} \tag{7-4}$$

Therefore, in the continuous-conduction mode, the step-down converter is equivalent to a dc transformer where the turns ratio of this equivalent transformer can be continuously controlled electronically in a range of 0–1 by controlling the duty ratio of the switch.

We observe that even though the average input current I_d follows the transformer relationship, the instantaneous input current waveform jumps from a peak value to zero every time the switch is turned off. An appropriate filter at the input may be required to eliminate the undesirable effects of the current harmonics.

7-3-2 BOUNDARY BETWEEN CONTINUOUS AND DISCONTINUOUS CONDUCTION

In this section, we will develop equations that show the influence of various circuit parameters on the conduction mode of the inductor current (continuous or discontinuous). At the edge of the continuous-current-conduction mode, Fig. 7-6*a* shows the waveforms for v_L and i_L. Being at the boundary between the continuous and the discontinuous mode, by definition, the inductor current i_L goes to zero at the end of the off period.

At this boundary, the average inductor current, where the subscript B refers to the boundary, is

$$I_{LB} = \frac{1}{2} i_{L,\text{peak}} = \frac{t_{on}}{2L}(V_d - V_o) = \frac{DT_s}{2L}(V_d - V_o) = I_{oB} \tag{7-5}$$

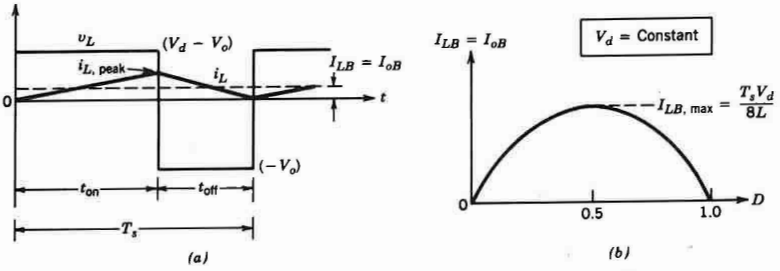

Figure 7-6 Current at the boundary of continuous–discontinuous conduction: (*a*) current waveform; (*b*) I_{LB} versus D keeping V_d constant.

Therefore, during an operating condition (with a given set of values for T_s, V_d, V_o, L, and D), if the average output current (and, hence, the average inductor current) becomes less than I_{LB} given by Eq. 7-5, then i_L will become discontinuous.

7-3-3 DISCONTINUOUS-CONDUCTION MODE

Depending on the application of these converters, either the input voltage V_d or the output voltage V_o remains constant during the converter operation. Both of these types of operation are discussed below.

7-3-3-1 Discontinuous-Conduction Mode with Constant V_d

In an application such as a dc motor speed control, V_d remains essentially constant and V_o is controlled by adjusting the converter duty ratio D.

Since $V_o = DV_d$, the average inductor current at the edge of the continuous-conduction mode from Eq. 7-5 is

$$I_{LB} = \frac{T_s V_d}{2L} D(1 - D) \tag{7-6}$$

Using this equation, we find that Fig. 7-6*b* shows the plot of I_{LB} as a function of the duty ratio D, keeping V_d and all other parameters constant. It shows that the output current required for a continuous-conduction mode is maximum at $D = 0.5$:

$$I_{LB,\max} = \frac{T_s V_d}{8L} \tag{7-7}$$

From Eqs. 7-6 and 7-7

$$I_{LB} = 4I_{LB,\max} D(1 - D) \tag{7-8}$$

Next the voltage ratio V_o/V_d will be calculated in the discontinuous mode. Let us assume that initially the converter is operating at the edge of continuous conduction, as in Fig. 7-6*a*, for given values of T, L, V_d, and D. If these parameters are kept constant and the output load power is decreased (i.e., the load resistance goes up), then the average inductor current will decrease. As is shown in Fig. 7-7, this dictates a higher value of V_o than before and results in a discontinuous inductor current.

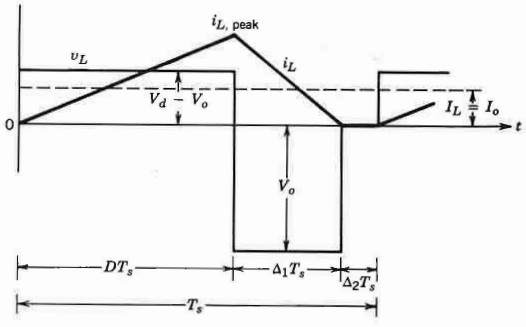

Figure 7-7 Discontinuous conduction in step-down converter.

During the interval $\Delta_2 T_s$ where the inductor current is zero, the power to the load resistance is supplied by the filter capacitor alone. The inductor voltage v_L during this interval is zero. Again, equating the integral of the inductor voltage over one time period to zero yields

$$(V_d - V_o)\, DT_s + (-V_o)\Delta_1 T_s = 0 \tag{7-9}$$

$$\therefore \frac{V_o}{V_d} = \frac{D}{D + \Delta_1} \tag{7-10}$$

where $D + \Delta_1 < 1.0$. From Fig. 7-7,

$$i_{L,\text{peak}} = \frac{V_o}{L}\Delta_1 T_s \tag{7-11}$$

Therefore,

$$I_o = i_{L,\text{peak}} \frac{D + \Delta_1}{2} \tag{7-12}$$

$$= \frac{V_o T_s}{2L}(D + \Delta_1)\,\Delta_1 \quad \text{(using Eq. 7-11)} \tag{7-13}$$

$$= \frac{V_d T_s}{2L} D\Delta_1 \quad \text{(using Eq. 7-10)} \tag{7-14}$$

$$= 4I_{LB,\max} D\Delta_1 \quad \text{(using Eq. 7-7)} \tag{7-15}$$

$$\therefore \Delta_1 = \frac{I_o}{4I_{LB,\max} D} \tag{7-16}$$

From Eqs. 7-10 and 7-16

$$\frac{V_o}{V_d} = \frac{D^2}{D^2 + \frac{1}{4}(I_o/I_{LB,\max})} \tag{7-17}$$

Figure 7-8 shows the step-down converter characteristic in both modes of operation for a constant V_d. The voltage ratio (V_o/V_d) is plotted as a function of $I_o/I_{LB,\max}$ for various values of duty ratio using Eqs. 7-3 and 7-17. The boundary between the continuous and the discontinuous mode, shown by the dashed curve, is established by Eq. 7-3 and 7-8.

7-3-3-2 Discontinuous-Conduction Mode with Constant V_o

In applications such as regulated dc power supplies, V_d may fluctuate but V_o is kept constant by adjusting the duty ratio D.

Since $V_d = V_o/D$, the average inductor current at the edge of the continuous-conduction mode from Eq. 7-5 is

$$I_{LB} = \frac{T_s V_o}{2L}(1 - D) \tag{7-18}$$

Equation 7-18 shows that if V_o is kept constant, the maximum value of I_{LB} occurs at $D = 0$:

$$I_{LB,\max} = \frac{T_s V_o}{2L} \tag{7-19}$$

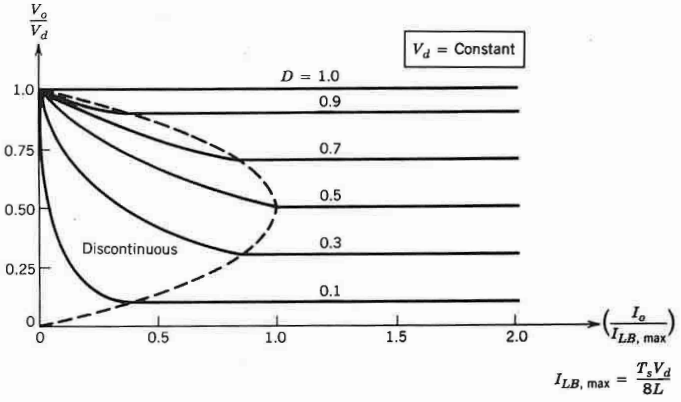

Figure 7-8 Step-down converter characteristics keeping V_d constant.

It should be noted that the operation corresponding to $D = 0$ and a finite V_o is, of course, hypothetical because it would require V_d to be infinite.

From Eqs. 7-18 and 7-19

$$I_{LB} = (1 - D)I_{LB,\max} \tag{7-20}$$

For the converter operation where V_o is kept constant, it will be useful to obtain the required duty ratio D as a function of $I_o/I_{LB,\max}$. Using Eqs. 7-10 and 7-13 (which are valid in the discontinuous-conduction mode whether V_o or V_d is kept constant) along with Eq. 7-19 for the case where V_o is kept constant yields

$$D = \frac{V_o}{V_d}\left(\frac{I_o/I_{LB,\max}}{1 - V_o/V_d}\right)^{1/2} \tag{7-21}$$

The duty ratio D as a function of $I_o/I_{LB,\max}$ is plotted in Fig. 7-9 for various values of V_d/V_o, keeping V_o constant. The boundary between the continuous and the discontinuous mode of operation is obtained by using Eq. 7-20.

7-3-4 OUTPUT VOLTAGE RIPPLE

In the previous analysis, the output capacitor is assumed to be so large as to yield $v_o(t) = V_o$. However, the ripple in the output voltage with a practical value of capacitance can be calculated by considering the waveforms shown in Fig. 7-10 for a continuous-conduction mode of operation. Assuming that all of the ripple component in i_L flows through the capacitor and its average component flows through the load resistor, the shaded area in Fig. 7-10 represents an additional charge ΔQ. Therefore, the peak-to-peak voltage ripple ΔV_o can be written as

$$\Delta V_o = \frac{\Delta Q}{C} = \frac{1}{C}\frac{1}{2}\frac{\Delta I_L}{2}\frac{T_s}{2}$$

From Fig. 7-5 during t_{off}

$$\Delta I_L = \frac{V_o}{L}(1 - D)T_s \tag{7-22}$$

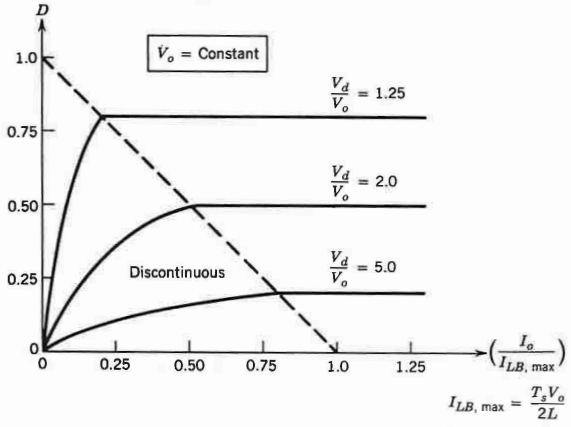

Figure 7-9 Step-down converter characteristics keeping V_o constant.

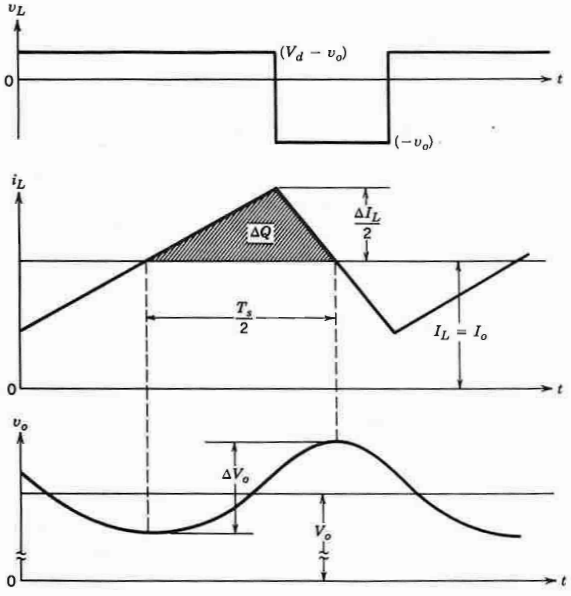

Figure 7-10 Output voltage ripple in a step-down converter.

Therefore, substituting ΔI_L from Eq. 7-22 into the previous equation gives

$$\Delta V_o = \frac{T_s}{8C}\frac{V_o}{L}(1 - D)T_s \tag{7-23}$$

$$\therefore \frac{\Delta V_o}{V_o} = \frac{1}{8}\frac{T_s^2(1 - D)}{LC} = \frac{\pi^2}{2}(1 - D)\left(\frac{f_c}{f_s}\right)^2 \tag{7-24}$$

where switching frequency $f_s = 1/T_s$ and

$$f_c = \frac{1}{2\pi\sqrt{LC}} \tag{7-25}$$

Equation 7-24 shows that the voltage ripple can be minimized by selecting a corner frequency f_c of the low-pass filter at the output such that $f_c \ll f_s$. Also, the ripple is independent of the output load power, so long as the converter operates in the continuous-conduction mode. A similar analysis can be performed for the discontinuous-conduction mode.

We should note that in switch-mode dc power supplies, the percentage ripple in the output voltage is usually specified to be less than, for instance, 1%. Therefore, the analysis in the previous sections assuming $v_o(t) = V_o$ is valid. It should be noted that the output ripple in Eq. 7-24 is consistent with the discussion of the low-pass filter characteristic in Fig. 7-4*c*.

7-4 STEP-UP (BOOST) CONVERTER

Figure 7-11 shows a step-up converter. Its main application is in regulated dc power supplies and the regenerative braking of dc motors. As the name implies, the output voltage is always greater than the input voltage. When the switch is on, the diode is reversed biased, thus isolating the output stage. The input supplies energy to the inductor. When the switch is off, the output stage receives energy from the inductor as well as from the input. In the steady-state analysis presented here, the output filter capacitor is assumed to be very large to ensure a constant output voltage $v_o(t) \simeq V_o$.

7-4-1 CONTINUOUS-CONDUCTION MODE

Figure 7-12 shows the steady-state waveforms for this mode of conduction where the inductor current flows continuously [$i_L(t) > 0$].

Since in steady state the time integral of the inductor voltage over one time period must be zero,

$$V_d t_{on} + (V_d - V_o)t_{off} = 0$$

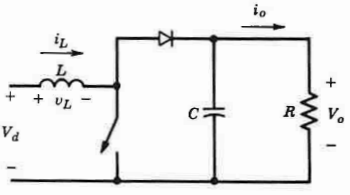

Figure 7-11 Step-up dc–dc converter.

The presence of the right-half zero can be explained by noting that in a flyback converter operating in a continuous mode, if the duty ratio d is increased instantaneously, the output voltage decreases momentarily because the inductor current has not had the time to increase, but the time interval $(1 - d)T_s$ during which the inductor transfers energy to the output stage has been suddenly decreased. This initial decline in the output voltage with the increase in d is opposite of what eventually takes place. This effect results in a zero in the right-half plane, which introduces phase lag in the transfer function $\tilde{v}_o(s)/\tilde{d}(s)$.

In a flyback converter operating in a discontinuous mode, the foregoing effect does not occur and the output voltage always increases with the increased duty ratio. Therefore, in the discontinuous mode of operation, the right-half-plane zero in the transfer function of Eq. 10-86 does not exist; thus, compensating the feedback loop to provide enough gain and phase margins is simpler.

10-5-2 TRANSFER FUNCTION $\tilde{d}(s)/\tilde{v}_c(s)$ OF THE DIRECT DUTY RATIO PULSE-WIDTH MODULATOR

In the direct duty ratio pulse-width modulator, the control voltage $v_c(t)$, which is the output of the error amplifier, is compared with a repetitive waveform $v_r(t)$, which establishes the switching frequency f_s, as shown in Fig. 10-23*a*. The control voltage $v_c(t)$ consists of a dc component and a small ac perturbation component

$$v_c(t) = V_c + \tilde{v}_c(t) \tag{10-87}$$

where $v_c(t)$ is in a range between zero and $\hat{V}_r$, as shown in Fig. 10-23*a*. Here $\tilde{v}_c(t)$ is a sinusoidal ac perturbation in the control voltage at a frequency ω, where ω is much smaller than the switching frequency ω_s $(=2\pi f_s)$. The ac perturbation in the control voltage can be expressed as

$$\tilde{v}_c(t) = a \sin(\omega t - \phi) \tag{10-88}$$

by means of an amplitude a and an arbitrary phase angle ϕ.

In Fig. 10-23*b*, the instantaneous switch duty ratio $d(t)$ is as follows:

$$d(t) = \begin{cases} 1.0 & \text{if } v_c(t) \geq v_r(t) \quad (10\text{-}89) \\ 0 & \text{if } v_c(t) < v_r(t) \quad (10\text{-}90) \end{cases}$$

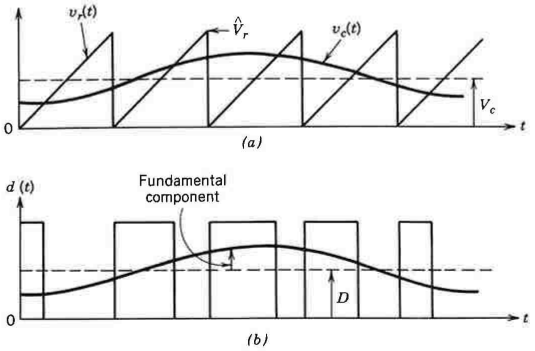

Figure 10-23 Pulse-width modulator.

Similar to the analysis of sinusoidal PWM carried out in Chapter 8, $d(t)$ in Fig. 10-23*b* can be expressed in terms of the Fourier series as

$$d(t) = \frac{V_c}{\hat{V}_r} + \frac{a}{\hat{V}_r}\sin(\omega t - \phi) + \text{other high-frequency components} \qquad (10\text{-}91)$$

The higher frequency components in the output voltage v_o due to the high-frequency components in $d(t)$ are eliminated because of the low-pass filter at the output of the converter. Therefore, the high-frequency components in Eq. 10-91 can be ignored. In terms of its dc value and its ac perturbation

$$d(t) = D + \tilde{d}(t) \qquad (10\text{-}92)$$

Comparing Eqs. 10-91 and 10-92 yields

$$D = \frac{V_c}{\hat{V}_r} \qquad (10\text{-}93)$$

and

$$\tilde{d}(t) = \frac{a}{\hat{V}_r}\sin(\omega t - \phi) \qquad (10\text{-}94)$$

From Eqs. 10-88 and 10-94, the transfer function $T_m(s)$ of the modulator is given by

$$T_m(s) = \frac{\tilde{d}(s)}{\tilde{v}_c(s)} = \frac{1}{\hat{V}_r} \qquad (10\text{-}95)$$

Therefore, the theoretical transfer function of the pulse-width modulator is surprisingly simple, without any time delays. However, the time delay associated with the comparator can lead to a delay in the modulator response.

■ ***Example 10-2*** In practice, the transfer function of the modulator may not have to be calculated from Eq. 10-95. Figure 10-24 shows the approximate transfer function of a commonly used PWM integrated circuit, supplied as a part of the data sheets, in terms of the duty ratio d as a function of the control voltage v_c, where v_c is the output of the error amplifier.

Calculate the transfer function $\tilde{d}(s)/\tilde{v}_c(s)$ for this PWM integrated circuit.

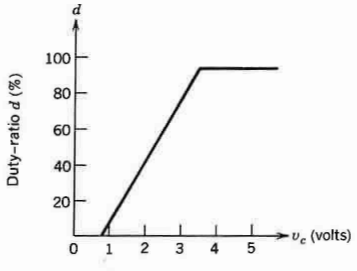

Figure 10-24 Pulse-width modulator transfer function.

Solution For this particular modulator, the duty ratio d increases from 0 (at $v_c = 0.8$ V) to 0.95 (at $v_c = 3.6$ V). Therefore, the slope of the transfer function in Fig. 10-24 is equal to the transfer function of this modulator:

$$\frac{\bar{d}(s)}{\bar{v}_c(s)} = \frac{\Delta d}{\Delta v_c} = \frac{0.95 - 0}{3.6 - 0.8} \simeq 0.34 \tag{10-96}$$

With this modulator, the transfer function between v_o and the control voltage v_c can be obtained as

$$T_1(s) = \frac{\bar{v}_o(s)}{\bar{v}_c(s)} = \frac{\bar{v}_o(s)}{\bar{d}(s)} \frac{\bar{d}(s)}{\bar{v}_c(s)} = T_p(s)T_m(s) \tag{10-97}$$

The gain plot of the transfer function $\bar{v}_o(s)/\bar{v}_c(s)$ can be obtained by adjusting the gain curve in the Bode plot of Fig. 10-21*a* or Fig. 10-22*a* to account for a constant gain of 0.34 (= −9.37 dB) of the modulator. Assuming zero delay in the modulator, the phase plot of $\bar{v}_o(s)/\bar{v}_c(s)$ is the same as that of $\bar{v}_o(s)/\bar{d}(s)$. ■

10-5-3 COMPENSATION OF THE FEEDBACK SYSTEM USING A DIRECT DUTY RATIO PULSE-WIDTH MODULATOR

In the switch-mode power supply shown in Fig. 10-19*b*, the overall open-loop transfer function is

$$T_{OL}(s) = T_1(s)T_c(s) \tag{10-98}$$

where $T_1(s)$ is as given by Eq. 10-97 and

$$T_c(s) = \text{transfer function of compensated error amplifier} \tag{10-99}$$

For a given $T_1(s)$, the transfer function of the compensated error amplifier $T_c(s)$ must be properly tailored so that $T_{OL}(s)$ meets the performance requirements expected of the power supply. Some of the desired characteristics of the open-loop transfer function $T_{OL}(s)$ are as follows:

1. The gain at low frequencies should be high to minimize the steady-state error in the power supply output.
2. The crossover frequency is the frequency at which the gain of $T_{OL}(s)$ falls to 1.0 (0 dB), as shown in Fig. 10-25. This crossover frequency ω_{cross} should be as high as possible but approximately an order of magnitude below the switching frequency to allow the power supply to respond quickly to the transients, such as a sudden change of load.
3. The phase margin (PM) is defined by means of Fig. 10-25 as

$$PM = \phi_{OL} + 180° \tag{10-100}$$

where ϕ_{OL} is the phase angle of $T_{OL}(s)$ at the crossover frequency and is negative. The phase margin, which should be a positive quantity in Eq. 10-100, determines the transient response of the output voltage in response to sudden changes in the load and the input voltage. A phase margin in a range of 45°–60° is desirable.

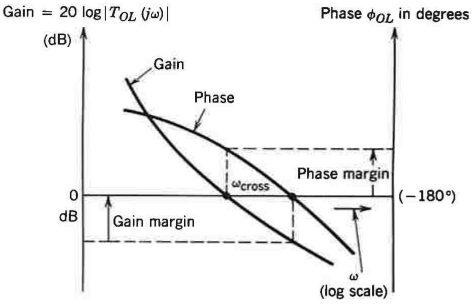

Figure 10-25 Gain and phase margins.

To meet these requirements simultaneously, a general error amplifier is shown in Fig. 10-26, where the amplifier can be assumed to be ideal. One of the inputs to the amplifier is the output voltage v_o of the converter; the other input is the desired (reference) value V_{ref} of v_o. The output of the error amplifier is the control voltage v_c. In terms of Z_i and Z_f in Fig. 10-26, the transfer function between the input and the output perturbations can be obtained as

$$\frac{\tilde{v}_c(s)}{\tilde{v}_o(s)} = -\frac{Z_f(s)}{Z_i(s)} = -T_c(s) \tag{10-101}$$

where $T_c(s)$ is as defined in Fig. 10-19*b*.

One of the options in the selection of $T_c(s)$ is to introduce a pole-zero pair in addition to a pole at the origin so that $T_c(s)$ is of the form

$$T_c(s) = \frac{A\ (s + \omega_z)}{s\ (s + \omega_p)} \tag{10-102}$$

where A is positive and $\omega_z < \omega_p$. In Eq. 10-102, due to the pole at the origin, the phase of $T_c(s)$ starts with $-90°$, as shown in Fig. 10-27*a*. The presence of the zero causes the phase angle to increase (or in other words provides a "boost") to be something greater than $-90°$. Eventually, because of the pole at ω_p, the phase angle of $T_c(s)$ comes back down to $-90°$. The gain plot is also shown in Fig. 10-27*a*. The parameters in Eq. 10-102 can be chosen such that the minimum phase lag in $T_c(s)$ occurs at the specified (desired) crossover frequency of the overall open-loop transfer function $T_{OL}(s)$.

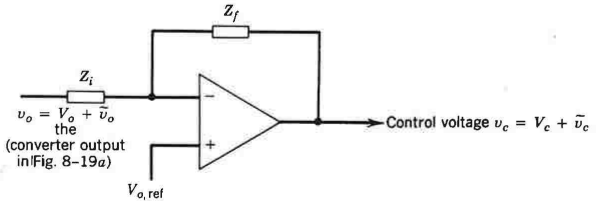

Figure 10-26 A general compensated error amplifier.

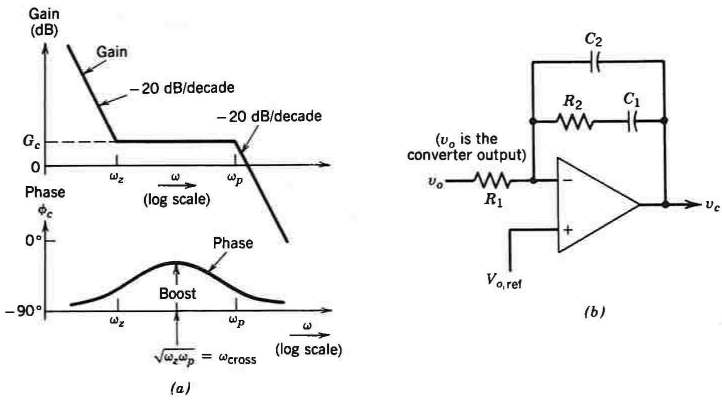

Figure 10-27 Error amplifier.

$$T_c(s) = \frac{1}{R_1C_2}\frac{s + \omega_z}{s(s + \omega_p)}$$

The transfer function in Eq. 10-102 can be realized by means of the amplifier network shown in Fig. 10-27*b*, where

$$T_c(s) = \frac{1}{R_1C_2}\frac{s + \omega_z}{s(s + \omega_p)} \tag{10-103}$$

$$\omega_z = \frac{1}{R_2C_1} \tag{10-104}$$

$$\omega_p = \frac{C_1 + C_2}{R_2C_1C_2} \tag{10-105}$$

A step-by-step explanation that is easy to follow in the selection of the foregoing parameters has been provided in reference 16 using a K-factor approach. This procedure suggests that as a first-step, the crossover frequency ω_{cross}, where $|T_{OL}(s)|$ would equal 0 dB, should be selected. This crossover frequency also defines the frequency in Fig. 10-27*a*, where the minimum phase lag occurs in the transfer function of $T_c(s)$. The K factor is used such that in the transfer function $T_c(s)$ of Eq. 10-103

$$\omega_z = \frac{\omega_{cross}}{K} \tag{10-106}$$

$$\omega_p = K\omega_{cross} \tag{10-107}$$

It is shown in reference 16 that K in Eqs. 10-106 and 10-107 is related to the boost (defined in Fig. 10-27*a*) in the following manner:

$$K = \tan\left(45° + \frac{\text{boost}}{2}\right) \tag{10-108}$$

Therefore, the next step is to define the phase margin (PM) and, hence, the boost needed

from the error amplifier at the crossover frequency to calculate K in Eqs. 10-106 and 10-107. From the definition of phase margin in Eq. 10-100

$$PM = 180° + \phi_1 + \phi_c \tag{10-109}$$

where ϕ_c is the phase angle of $T_c(s)$ at the crossover frequency. From Eq. 10-97

$$\phi_1 = \phi_p(s) + \phi_m(s) \tag{10-110}$$

where ϕ_1 is the phase angle of $T_1(s)$, $\phi_p(s)$ is the phase angle of the power stage $T_p(s)$, and $\phi_m(s)$ is the phase angle (if any) of the modulator $T_m(s)$. From the phase plot of the transfer function $T_c(s)$ shown in Fig. 10-27*a*

$$\phi_c = -90° + \text{boost} \tag{10-111}$$

From Eqs. 10-109 and 10-111,

$$\text{boost} = \text{PM} - \phi_1 - 90° \tag{10-112}$$

Therefore, once the phase margin (usually in a range of 45°–60°) is chosen, the boost is defined from Eq. 10-112 where ϕ_1 (assuming ϕ_m to be zero) can be obtained from Fig. 10-21*b* or Fig. 10-22*b* at the frequency chosen to be the crossover frequency. Knowing the boost, K can be calculated from Eq. 10-108.

The next step in the design procedure is to ensure that the gain G_{OL} of the overall open-loop is equal to 1 (i.e., $G_{OL} = |T_{OL}(s)| = 1$) at the chosen crossover frequency. This requires that from Eq. 10-98, the gain G_c of the compensated error amplifier at ω_{cross} be as follows:

$$G_c(\text{at } \omega_{cross}) = \frac{1}{G_1(\text{at } \omega_{cross})} \tag{10-113}$$

where G_1 is the magnitude $|T_1(j\omega_{cross})|$ of the transfer function $T_1(s) = T_p(s)T_m(s)$ at ω_{cross}. Therefore, at $\omega = \omega_{cross}$, from Eq. 10-113 and by the substitution of Eqs. 10-104 through 10-107 into Eq. 10-103,

$$G_c = \frac{1}{KC_2R_1\omega_{cross}} = \frac{1}{G_1} \tag{10-114}$$

In the circuit of Fig. 10-27*b*, R_1 is chosen arbitrarily and the rest of the circuit parameters can be calculated as follows from the K-factor procedure outlined before using Eqs. 10-104 through 10-107 and Eq. 10-114,

$$C_2 = \frac{G_1}{KR_1\omega_{cross}} \tag{10-115}$$

$$C_1 = C_2(K^2 - 1) \tag{10-116}$$

$$R_2 = \frac{K}{(C_1\omega_{cross})} \tag{10-117}$$

For the converters, such as a flyback converter operating in a continuous mode, it may be necessary to use an error amplifier that has two pairs of poles and zeros in addition to the pole at the origin for a proper compensation.

10-5-4 VOLTAGE FEED-FORWARD PWM CONTROL

In the direct duty ratio PWM control discussed in the previous two sections, if the input voltage changes, an error is produced in the output voltage, which eventually gets cor-

rected by the feedback control. This results in a slow dynamic performance in regulating the output in response to the changes in input voltage.

If the duty ratio could be adjusted directly to accommodate the change in the input voltage, then the converter output would remain unchanged. This can be accomplished by feeding the input voltage level to the PWM IC. The PWM switching strategy here is very similar to the one discussed in connection with the direct duty ratio PWM control except for one difference: the ramp (and, hence, the peak) of the sawtooth waveform does not stay constant but varies in direct proportion to the input voltage, as shown in Fig. 10-28. This shows how an increased input voltage (hence, increased $\hat{V}_r$) results in a decreased duty ratio, shown by dashed curves in Fig. 10-28. This type of control in step-down derived converters (e.g., forward converters) results in $\bar{v}_o(s)/\bar{v}_d(s)$ equal to zero and hence in an excellent inherent regulation for the changes in the input voltage. The same is true for a flyback converter operating in a complete demagnetization mode.

If this voltage feed-forward is implemented in a double-ended power supply (like push–pull, half-bridge, full bridge), then care must be taken to provide a dynamic volt–time balance so that the on times of the two switches are kept equal on a dynamic basis to prevent the saturation of the high-frequency isolation transformer.

10-5-5 CURRENT-MODE CONTROL

The PWM direct duty ratio control discussed so far is shown in Fig. 10-29*a*, where the control voltage v_c (amplified error signal between the actual output and the reference) controls the duty ratio of the switch by comparing the control voltage with a fixed-frequency sawtooth waveform. This control of the switch duty ratio adjusts the voltage across the inductor and hence the inductor current (which feeds the output stage) and eventually brings the output voltage to its reference value.

In a current-mode control, an additional inner control loop is used as shown in Fig. 10-29*b*, where the control voltage v_c directly controls the output inductor current that feeds the output stage and thus the output voltage. Ideally, the control voltage should act to directly control the *average* value of the inductor current for the fastest response, though, as we will see later, various types of current-mode controls tend to accomplish this differently. The fact that the current feeding the output stage is controlled directly in a current-mode control has a profound effect on the dynamic behavior of the negative-feedback control loop.

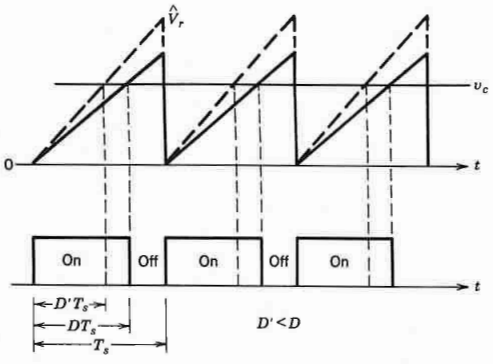

Figure 10-28 Voltage feed-forward: effect on duty ratio.

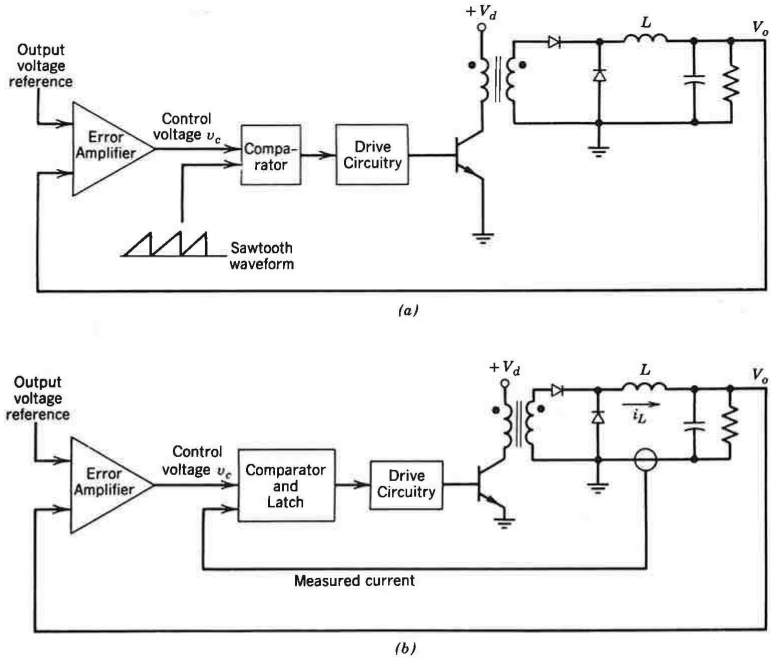

Figure 10-29 PWM duty ratio versus current-mode control: (*a*) PWM duty ratio control; (*b*) current-mode control.

There are three basic types of current-mode controls:

1. Tolerance band control
2. Constant-"off"-time control
3. Constant-frequency control with turn-on at clock time

In all these types of controls, either the inductor current or the switch current, which is proportional to the output inductor current, is measured and compared with the control voltage.

In the *tolerance band control,* the control voltage v_c dictates the average value of the inductor current as shown in Fig. 10-30*a*. The term ΔI_L is a design parameter. The switching frequency depends on ΔI_L, the converter parameters, and the operating conditions. This direct control over the average value of i_L is a very desirable feature of this type of control. However, this scheme works well only in the continuous-current-conduction mode. Otherwise, in the discontinuous-current-conduction mode, the inductor current becomes zero (though $\frac{1}{2}\Delta I_L$ would actually be demanding a negative i_L, which is not possible). If the controller is not designed to handle this discontinuous current when i_L is zero and i_L being demanded by the controller is negative, the switch will never turn on and the inductor current will decay to zero.

In the *constant-off-time control*, the control voltage dictates $\hat{I}_L$, as is shown in Fig. 10-30*b*. Once $\hat{I}_L$ is reached, the switch turns off for a fixed (constant) off time, which is

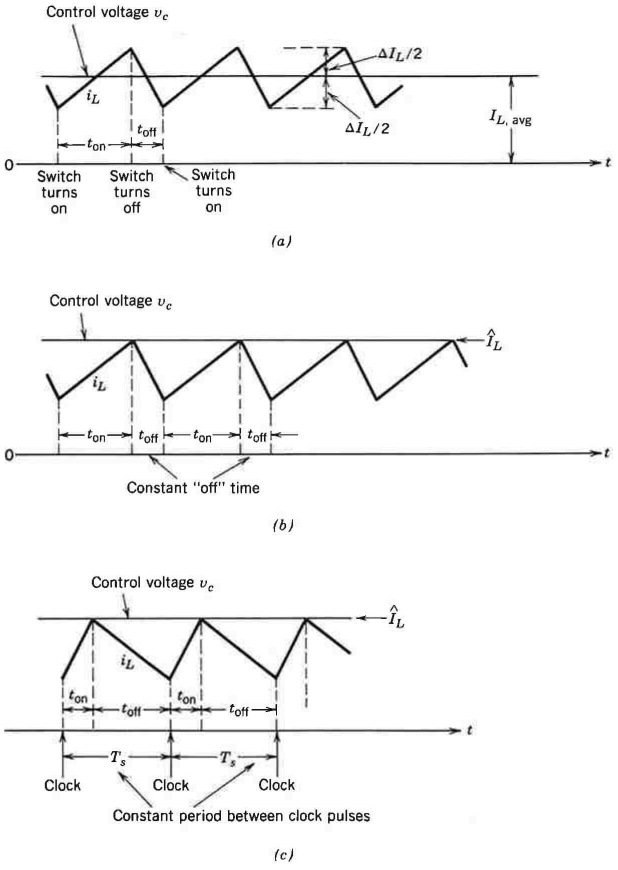

Figure 10-30 Three types of current-mode control: (*a*) tolerance band control; (*b*) constant-off-time control; (*c*) constant frequency with turn-on at clock time.

a design parameter. Here also, the switching frequency is not fixed and depends on the converter parameters and its operating condition.

The *constant-frequency control with a turn-on at clock time* is thus far the most common type of current-mode control. Here, the switch is turned on at the beginning of each constant-frequency switching time period. The control voltage dictates $\hat{I}_L$ and the instant at which the switch is turned off, as shown in Fig. 10-30*c*. The switch remains off until the beginning of the next switching cycle. A constant switching frequency makes it easier to design the output filter.

In the current-mode control in practice, a slope compensation is added to the control voltage, as shown in Fig. 10-31, to provide stability, to prevent subharmonic oscillations, and to provide a feed-forward property. Figure 10-31 shows the waveforms for a forward

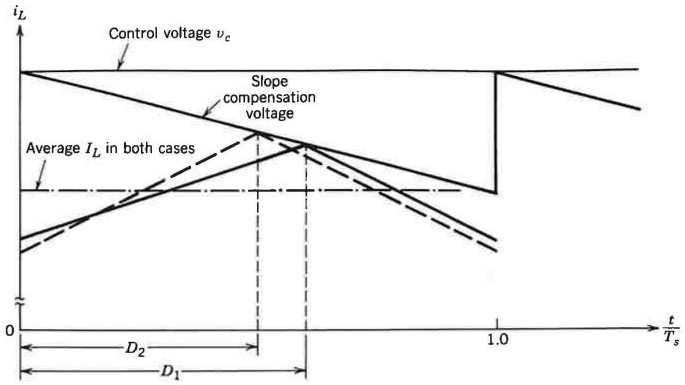

Figure 10-31 Slope compensation in current-mode control (D_2 is smaller for a higher input voltage with a constant V_o).

converter of the type shown in Fig. 10-29*b*, where the slope of the slope compensation waveform is one-half of the slope of the inductor current when the switch is off. With given input and output voltages, the duty ratio is D_1 and the waveform of the inductor current i_L is shown by the solid lines. If the input voltage is increased but the output voltage is to remain unaffected, the duty ratio decreases to D_2 and the inductor current waveform is shown by dashed lines. The average value of the inductor current, which equals the load current, remains the same in both cases in spite of a change in the input voltage. This shows the voltage feed-forward property of the current-mode control with a proper slope compensation.

The current-mode control has several advantages over the conventional direct duty ratio PWM control:

1. *It limits peak switch current.* Since either the switch current is directly measured or the current is measured somewhere in the circuit (like through the output inductor) where it represents the switch current without delay, the peak value of the switch current can be limited by simply putting an upper limit on the control voltage. This can be easily accomplished in the controllers that control $\hat{I}_L$.
2. *It removes one pole* (corresponding to the output filter inductor) from the control-to-output transfer function $\tilde{v}_o(s)/\tilde{v}_c(s)$, thus simplifying the compensation in the negative-feedback system, especially in the presence of the right-half-plane zero.
3. It allows a *modular design* of power supplies by equal current sharing where several power supplies can be operated in parallel and provide equal currents, if the same control voltage is fed to all the modules.
4. It results in a *symmetrical flux excursion* in a push–pull converter, thus eliminating the problem of transformer core saturation.
5. *It provides input voltage feed-forward.* As shown by Fig. 10-31, an input voltage feed-forward is automatically accomplished, resulting in an excellent rejection of input line transients.